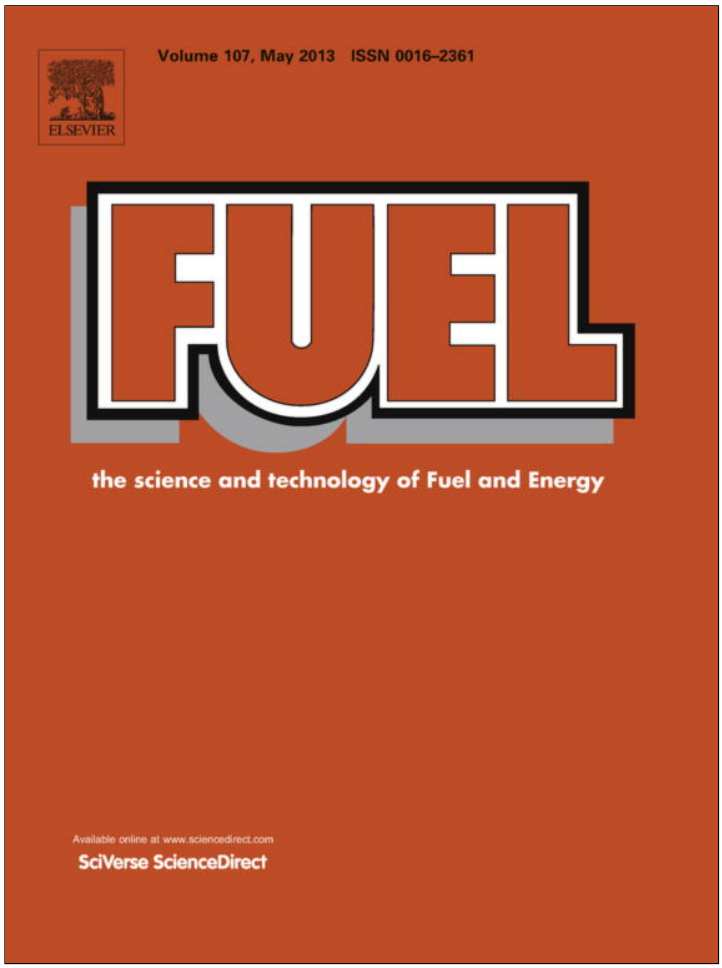

Fuel 107 (2013) 623–632

Contents lists available at SciVerse ScienceDirect

Fuel

journal homepage: www.elsevier.com/locate/fuel

The interplay of phase equilibria and chemical kinetics in a liquid/liquid multiphase biodiesel reactor

Michael Pomykala [a], James D. Stuart [b], Iman Noshadi [a], Richard S. Parnas [a,b,c,*]

[a] Chemical & Biomolecular Engineering Dept., University of Connecticut, United States
[b] Chemistry Dept., University of Connecticut, United States
[c] Institute of Materials Science, University of Connecticut, United States

HIGHLIGHTS

- Countercurrent liquid/liquid phase biodiesel reactor.
- Distributed methanol injection strategy.
- Improve reactor performance, yielding ASTM quality biodiesel and 90% separation efficiencies.
- A model that simulates the experimental results and provides insight into the reactor behavior.

ARTICLE INFO

Article history:
Received 2 September 2012
Received in revised form 20 November 2012
Accepted 2 December 2012
Available online 20 December 2012

Keywords:
Biodiesel
Reactor
Separator
Model
ASTM

ABSTRACT

A countercurrent liquid/liquid phase biodiesel reactor achieved 99% triglyceride to methyl ester conversion at the same time as separating 90% of the produced glycerin. However, a low inverse sensitivity of the conversion to the glycerin separation efficiency led to biodiesel that did not meet ASTM quality standards in previous work. A distributed methanol injection strategy is demonstrated herein to improve reactor performance, yielding ASTM quality biodiesel and 90% separation efficiencies. Preliminary data on feed rate changes yields counterintuitive results where conversion increases as feed rate increases. A model that assumes equilibrium between the reacting oil phase and the settling glycerol phase simulates the experimental results and provides insight into the reactor behavior.

1. Introduction

1.1. Background

Alternative renewable fuels are becoming increasingly important due to diminishing petroleum reserves and the negative environmental impact of fossil fuels. Numerous studies have shown that triglycerides, including virgin vegetable oil, waste vegetable oil, and animal fats can be converted into promising alternatives for diesel engine fuels via transesterification [1–4].

The chemical processing strategy for the production of biodiesel originated in the 1940s [5,6] and currently biodiesel production via base catalyzed transesterification is mainly performed using batch processes on small scales although new technologies are being developed for continuous processing including continuously stirred tank reactors [7], turbulent flow tubular reactors [8], re-circulating reactors containing long pathways of static mixers [9], and sub- and supercritical processes [10].

The overall reaction scheme for the methanolysis of triglycerides, illustrated in Scheme 1, is comprised of three sequential reactions.

$$TG + MeOH \rightleftharpoons DG + FAME \quad (R.1)$$

$$DG + MeOH \rightleftharpoons MG + FAME \quad (R.2)$$

$$MG + MeOH \rightleftharpoons G + FAME \quad (R.3)$$

where triglycerides, diglycerides, monoglycerides, methyl esters, and glycerin are represented by *TG*, *DG*, *MG*, *FAME*, and *G* respectively. The conversion can be enhanced by the continuous removal of the products during the reaction. While there are several current

* Corresponding author. Address: Institute of Materials Science, University of Connecticut, Storrs, CT 06269, United States. Tel.: +1 860 486 9060.
E-mail address: rparnas@ims.uconn.edu (R.S. Parnas).

0016-2361/$ - see front matter © 2012 Elsevier Ltd. All rights reserved.
http://dx.doi.org/10.1016/j.fuel.2012.12.017

strategies for simultaneously producing biodiesel and separating the glycerol phase [11–14], they require elevated temperatures and pressures and/or extra equipment for the separation process. A simpler combined process would decrease capital and operating costs.

There is a strong incentive to raise the conversion to 99% or above during the production of biodiesel, and that is the ASTM Standard definition of commercial grade biodiesel fuel, ASTM D6751. The chemical quality of the biodiesel is defined by a subtest of ASTM D6751, ASTM D6584-10a, called the free and total glycerin test. Free and total glycerin values are derived from a gas chromatography (GC) analysis of the fuel. The free glycerin measures the amount of glycerin byproduct left in the biodiesel, and is an assessment of how well the biodiesel has been purified of contaminants. The total glycerin combines the free glycerin and "bound glycerin", a nomenclature referring to remaining tri-, di-, and mono-glycerides in the biodiesel that were not converted to the methyl-esters via reactions R.1–R.3. To pass this ASTM test, the production process must remove the byproduct glycerin and attain a chemical conversion of approximately 99%. If the chemical conversion in the reactor is too low, expensive separation steps are required to sufficiently purify the biodiesel to pass the ASTM tests.

1.2. Laminar flow reactor/separator concept

The combination of liquid–liquid extraction with chemical reaction has long been used in processes ranging from metal recovery from leach liquors to aromatic nitrations to methyl acetate synthesis. The majority of literature published in this area, however, has been directed toward turbulent flow [15] and/or packed bed reactors [16] sometimes requiring multiple units [17]. The use of such a process for biodiesel production is unique in that the current reactor utilizes laminar flow in one column to simultaneously achieve very high conversion and separation.

In previous work, preliminary results with this reactor were introduced and performance questions were raised. In this paper, the performance of this laminar flow reactor/separator is examined under several operating conditions and a simple model proposed to explain the counterintuitive results obtained. In previous studies by others, it was shown that intense mixing is required to achieve high conversions in biodiesel production due to the limited miscibility of triglyceride oils and methanol [18]. The current reactor, however, takes advantage of the large change in miscibility that occurs once a small amount of the methyl ester product is formed. The reactor/separator has been proven to attain high conversion of triglycerides to methyl esters while separating more than 90% of the glycerol formed by reaction [19–21]. The reactor/separator contains an upward moving reacting phase that eventually exits the top of the reactor as biodiesel and a downward flowing raw glycerol phase that accumulates and exits at the bottom of the reactor/separator.

Unker et al. [21] examined the relationship between the gravity vector, the flow vector, and the reactor performance at various tilt angles, θ, of the reactor (Fig. 1). Glycerin separation efficiency showed strong dependence on the reactor angle. Only 35–50% of the glycerin separated from the reacting stream when the reactor was vertical, but 90% of the glycerin separated when the reactor was tilted to an angle of 30° from the horizontal. The conversion of triglycerides was observed to be insensitive to changes in reactor angle, decreasing from roughly 99% at 90° to 97% at 30° tilt angle. The produced biodiesel passed the ASTM D6584-10a free and total glycerin test when the reactor was vertical (90°) but failed the ASTM D6584-10a free and total glycerin test at tilt angles of 45° and 30°. Thus, a small change in the conversion attained in the reactor can have a major impact on the overall performance of the process.

It is hypothesized in this investigation that the decrease in conversion at tilted reactor orientations is caused by the increase in glycerin separation efficiency. As the glycerol byproduct stream flows countercurrently to the reacting mixture, it may scrub the methoxide from the reacting mixture. When the reactor is tilted and the glycerol flow increases substantially due to much higher separation efficiency, more methoxide may be removed from the upward flowing reacting mixture, resulting in less methoxide to interact with the vegetable oil than originally intended. One possible solution to this problem is to simply increase the methoxide injection rate, but that would decrease the overall efficiency of the reactor and place a larger waste load on the overall process. The proposed solution described below is to change the reactant injector design to divert some of the methoxide to a higher point in the reactor (Fig. 1) in an effort to alleviate the scrubbing problem, restore conversion to higher values, and allow the reactor to separate a large fraction of the glycerin that forms.

Injector design plays a vital role in reactor performance. The effect of geometrical positioning of injectors on reactor performance has been documented in processes ranging from nitride deposition during chemical vapor deposition [22] to gas hydrate formation [23]. Injector selection is particularly important in the current study due to the laminar flow in the reactor/separator. A static mixer was chosen for the primary injector to overcome miscibility limitations of methanol with triglycerides [20] and a countercurrent misting nozzle was chosen for secondary injection to disperse methoxide into the flow without disturbing the reacting flow.

2. Materials and methods

2.1. Equipment setup

As seen in the schematic in Fig. 2, the equipment consists of three major components; a glass reactor/separator, a methoxide mixing/storage tank, and a water heater. The reactor/separator, labeled 1 in Fig. 2, consists of a 1.2 m long glass column with a 0.15 m ID. Two brass caps enclose the ends of the tube and each is fitted with its respective injection unit. The primary injection unit is attached to the bottom end cap and consists of a 0.3 m length static mixer that leads to a 0.15 m length static mixer within the glass tube. A perforated metal disk covers the opening of the inner static mixer to disperse incoming flow radially. The top end-cap was fitted with an additional injection unit. This injection unit consists of a 0.35 m long stainless steel tube with a 3 mm ID. A stainless steel full-cone misting nozzle, with a 0.5 mm orifice, was mounted onto the end of the tube in order to disperse methoxide flow against the upward moving reacting flow.

Labeled 2 in Fig. 2 is the mixing/storage unit for the potassium hydroxide–methanol (methoxide) solution. It consists solely of a sealed 190 L PVC tank plumbed to supply methoxide to the reactor/separator. Labeled 3 in Fig. 2 is the 450 L water heater (Vanguard 240/280 V) used for heating the raw oil feedstock. The water heater is equipped with a 4.5 kW heating element and a thermostat for temperature control. The thermostat was too inaccurate for the experiments described below. Constant monitoring and manual control was required to keep the feed temperatures consistent throughout the experiment.

As indicated in Fig. 2, temperatures (T), liquid phase levels (L), and liquid flow rates (F) were measured at various locations. A National Instruments PCI-6221 DAQ board with a SCC-68 I/O connector block was used to record flows and temperatures at given time intervals. A LabVIEW control system with a PI algorithm in conjunction with the electronic proportional valves, V_{1A} and V_{2A}, controlled the flows of incoming methoxide and vegetable oil, respectively. Biodiesel was allowed to exit the top of the reactor

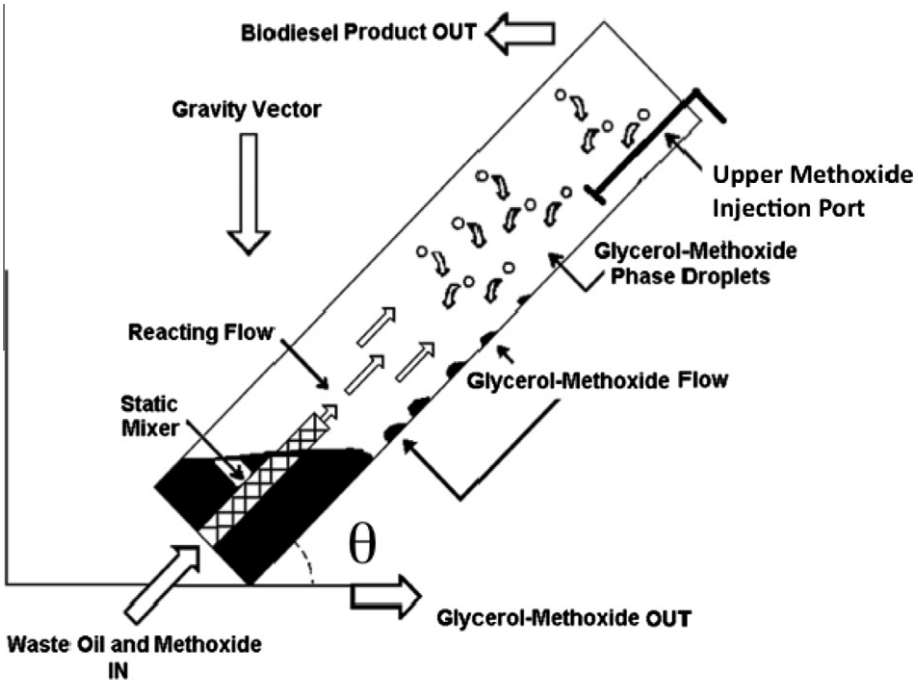

Fig. 1. Laminar flow reactor/separator operating concept.

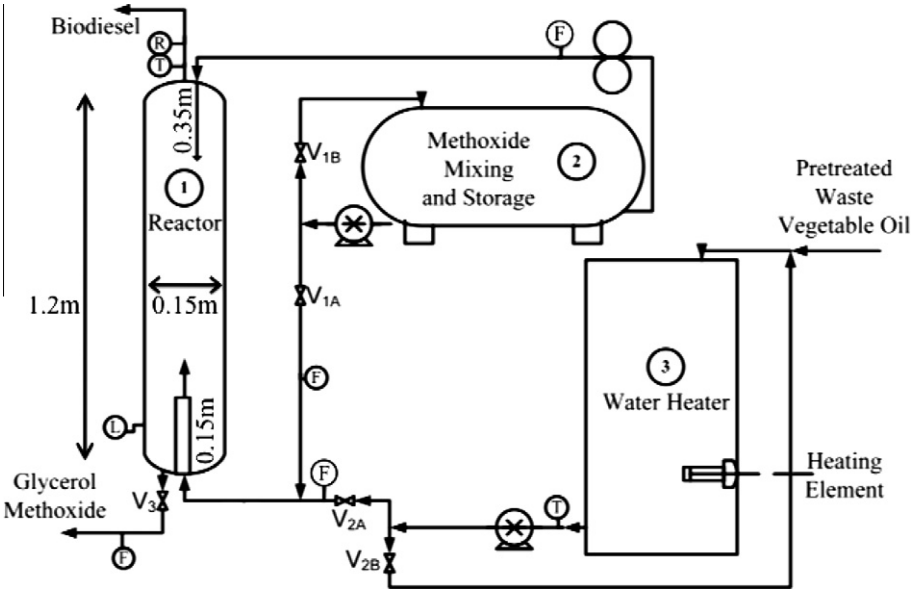

Fig. 2. Schematic diagram of reactor system.

at an uncontrolled rate while valve V_3 in Fig. 2 was used to manually adjust the exiting glycerol stream flow. Finally, the reactor was mounted on a hand-cart to facilitate tilting of the reactor to three preset angles (30°, 45°, 90°).

2.2. Feedstock preparation

Waste vegetable oil was collected from University of Connecticut dining halls. The waste vegetable oil was then filtered and pretreated via esterification in 50-gallon batches using a process documented previously [24]. All batches were then blended and titrated to measure a final free fatty acid (FFA) content of <0.5 wt%. All pretreated waste vegetable oil batches were then blended again to ensure a uniform feedstock for each experiment reported below.

Using waste vegetable oil for these experiments clearly introduces a degree of variability into the experiments, and that variability will be seen in the results below. Many investigations have documented the kinetics and thermodynamics of vegetable oil and biodiesel systems with pristine chemical constituents [25,26]. It is important to also document the performance of processing equipment and process designs with realistic feedstock in

order to verify that impurities do not adversely affect performance. The results presented below are designed to illustrate the performance to be expected with this reactor design under realistic operating conditions.

The pretreated waste vegetable oil was added to the water heater where it was circulated in full recycle by a positive displacement pump and preheated to roughly 50 °C. The remainder of the pretreated vegetable oil was placed into a similar water heater to be preheated to 50 °C, and stored for later replenishment of the feedstock in the 450 L water heater throughout the experiments. 150 L of methanol was added to the 190L storage tank and 12.5 kg of potassium hydroxide flakes (Oxychem 88 wt% Caustic Potash Anhydrous) were dissolved into the methanol over the course of 30 min. A motorized mechanical mixer was used to aid in the dissolution of potassium hydroxide flakes. Methoxide was replenished with small batches that were created using the same relative amounts of methanol and potassium hydroxide throughout the experiments.

2.3. Starting and running the reactor

The reactor/separator was primed with 21L of ASTM quality biodiesel at ambient temperature to facilitate a faster startup. Valves V_{1A} and V_{2A} were closed while valves V_{1B} and V_{2B} were open to allow reactants to be circulated in full recycle. V_{1A} and V_{2A} were then slightly opened to allow methoxide and vegetable oil to enter the reactor/separator. The LabVIEW system then adjusted valves V_{1A} and V_{2A} to attain desired flow rates of reactants into the reactor.

Each experiment reported below was performed as a series of segments. A segment of an experiment is a period of time during which the reactor tilt angle, feed rate, injection strategy, and other controllable variables were all held as nearly constant as possible. When a variable such as injection strategy or reactor tilt angle was changed, a new segment was started. The time period associated with each segment of an experiment is typically 3 h, although in one case a 2-h segment was used and in one case a segment was run for 4 h. The time period of the segment, after a change was made, was designed to allow the reactor to reach steady state operation so that reliable measurements of chemical conversion and glycerin separation efficiency could be obtained. An important point to note is that the reactor was not stopped between segments. During an experiment, the reactor was run continuously for the entire experiment, but one variable was changed as we proceeded from segment to segment.

2.4. Data collection

The LabVIEW control system was designed to record reactant inlet flows, glycerol outlet flow, and water heater and reactor exit temperatures at 1-min intervals. Valve V_3 was adjusted manually as needed to maintain a constant glycerol interface level within the reactor. After the first hour of operation, hourly manual density measurements were taken for the top and bottom exit streams of the reactor. Along with the hourly density samples, 50 mL samples were also taken of each exit stream for compositional analysis. The top samples were immediately quenched with 5 drops of 36% HCl (Sigma Aldrich reagent grade) and refrigerated to cease further chemical reaction. The bottom samples were immediately sealed and refrigerated to prevent evaporative loss of methanol.

Top sample analysis was performed via gas chromatography on a Hewlett Packard 5890 Series II gas chromatograph. The samples were first centrifuged to separate any residual glycerol. The methyl ester layer was drawn off and washed with water and dried over anhydrous sodium sulfate. The samples were then prepared and tested according to ASTM method D6584-10a to determine free and total glycerin, and mass percentages of triglycerides, diglycerides, and monoglycerides were also obtained. Gas chromatography was performed on each hourly top sample three times to obtain replicate data.

Bottom sample analysis was performed in two parts to analyze composition. First, thermogravimetric analysis (TGA) was performed to obtain the methanol mass fraction. Separate portions of each bottom sample were also titrated to determine the KOH composition using a standardized HCl solution. Titration solutions were prepared by mixing 0.5 g of sample with 30 mL of a titration solution composed of toluene, water, and isopropyl alcohol and titrated to completion using a phenolphthalein indicator. Titration and TGA analyses were performed on each hourly bottom sample 3 times to obtain replicate data.

2.5. Reactor performance

Reactor performance was assessed by calculating the conversion of *TG*, *DG*, and *MG* to *FAME* and also by calculating the glycerin (*G*) separation efficiency. The conversion, *X*, can be expressed by the following equation:

$$X = \frac{\{[TG]_0 + [DG]_0 + [MG]_0\} - \{[TG] + [DG] + [MG]\}}{\{[TG]_0 + [DG]_0 + [MG]_0\}} \quad (1)$$

where $[TG]_0$, $[DG]_0$, and $[MG]_0$ represent the tri-, di-, and mono-glycerides in the feedstock (mass/volume) and $[TG]$, $[DG]$, and $[MG]$ represent the tri-, di-, and mono-glycerides in the ester rich phase exiting the top of the reactor (mass/volume). Concentrations of the glycerides in the feedstock and the hourly samples from the top of the reactor were measured using gas chromatography as noted above.

Glycerin separation efficiency, G_E, was calculated using the following equation:

$$G_E = \frac{F_{GS}}{F_{GP}} \quad (2)$$

where the separation efficiency is equal to flow of glycerin leaving the bottom of the reactor/separator, F_{GS}, divided by the theoretical amount of glycerin produced by the reaction, F_{GP}.

The theoretical amount of glycerin being produced via the transesterification reaction, F_{GP}, was calculated using the following equation:

$$F_{GP} = \frac{F_O \rho_O}{MW_O} X\ MW_G \quad (3)$$

where F_{GP} is the mass production rate of glycerin by transesterification of the glycerides, F_o is the measured volumetric flow of oil feed, ρ_o is the measured density of the oil feed, X is the measured conversion, and MW_o and MW_G are the molecular weights of oil and glycerin, respectively. The contribution of diglycerides and monoglycerides to the oil feed molecular weight are neglected as they are present at well under 1 wt%. The basis of the theoretical glycerin equation is the stoichiometry of the transesterification reactions (R.1)–(R.3). These reactions require that one mole of glycerin be produced for each mole of triglycerides consumed. The chemical conversion presented in Eq. (1) provides an accurate estimate of the maximum amount of glycerin produced by reaction, F_{GP}.

The flow of glycerin leaving the bottom of the reactor/separator can be obtained from the total glycerol stream flow and the glycerin mass fraction as given by the following equation:

$$F_{GS} = F_G \rho_G (1 - y_{MeOH} - y_{KOH}) \quad (4)$$

where F_{GS} is the glycerin mass flow exiting the bottom of the reactor in the glycerol byproduct stream, F_G is the measured volumetric glycerol byproduct stream flow, ρ_G is the measured glycerol byproduct stream density, and y_{MeOH} and y_{KOH} are the measured methanol and KOH mass fractions in the glycerol stream, respectively. The

glycerin mass fraction, y_G, is obtained by assuming that the glycerol byproduct stream exiting the bottom of the reactor is composed of only glycerin, methanol and KOH, so that $y_G = 1 - y_{MeOH} - y_{KOH}$.

3. Results

The present study contains data from three separate experiments in which the reactor was operated using pretreated waste vegetable oil as the feedstock. The pretreated waste vegetable oil was heated to 50 °C and fed to the reactor at a nominal rate of 0.95 L/m, while ambient temperature methoxide at a concentration of 2 wt% KOH to triglycerides was fed to the reactor at a nominal rate of 0.22 L/m. The three experiments were all conducted in the same way for their first 3 segments, where the reactor was first run in a vertical orientation with no methoxide diversion ($D_M = 0$), and then at a 45° tilted orientation with $D_M = 0$, and then at a 45° tilted orientation with $D_M = 25\%$. Additional segments were run in experiments 2 and 3, and all the experiments are summarized in Table 1. Additional details about each individual experiment are provided below.

3.1. Experiment 1

The first experiment was performed in three segments, as noted in Table 1. In the third segment, the upper methoxide injection was turned onto a flow of 0.055 L/min, while the bottom methoxide injection flow was decreased to 0.165 L/min so that the total methoxide flow remained constant at 0.22 L/min, but 25% was diverted to the upper injector ($D_M = 25\%$).

Fig. 3 shows the conversion results from experiment 1 as calculated by Eq. (1) using GC measurements. In the first segment the conversion, X, is near 99%. In segment two X drops to approximately 98%. The third segment has conversions mostly over 99%. All samples from segments one and three passed the ASTM free and total glycerin test while nearly all samples from segment two failed (Table 2).

Table 2 presents the GC analysis results in terms of X (Eq. (1)) and in terms of the ASTM free and total glycerin test. Each GC run was individually analyzed, and the 3 runs at each hourly sampling are averaged for presentation in Table 2. This first experiment illustrates the critical importance of reactor performance since the roughly 1% decrease in X from segment 1 to segment 2 caused the produced biodiesel to fail the ASTM test, rendering it unfit for commercial sale. The third segment of the experiment illustrates the importance of design details, in this case the injection strategy, for maximizing reactor performance since diverting a portion of the methoxide to a second injection location increased performance substantially. While there are several alternative design and processing changes that may also achieve the required product quality goals, a rather simple change in injection design is probably the most cost effective.

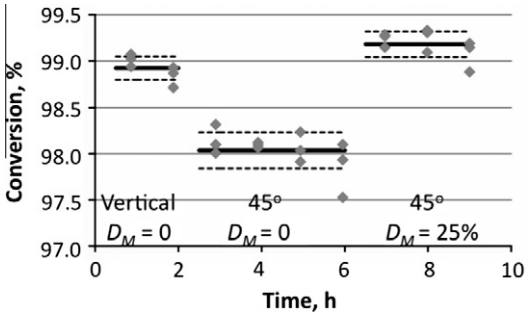

Fig. 3. Experiment 1. Conversion vs. Time. Each conversion data point is displayed, along with the average conversion attained during each segment of the experiment. The standard deviations of the data in each segment of the experiment are also displayed as dotted lines above and below the solid line representing the average value of the conversion.

The glycerin separation efficiency data were not collected at a large number of times in this experiment, but the average separation efficiency, G_E, for each segment was estimated from long term averaged flows and composition information (Table 3). The large increase in G_E observed when the reactor was tilted from vertical (segment 1) to a 45° angle (segment 2) is consistent with observations published previously [21]. Segment 3 indicates that $D_M = 25\%$ may cause a decrease in G_E, but the accuracy of this separation data is not good enough to draw any firm conclusions. The separation data in segments 1 and 3 have large uncertainties, indicating that the difference observed between segments 1 and 2 is probably significant, but the decrease in recovery observed in segment 3 may not be significant.

3.2. Experiment 2

Experiment 2 consisted of five segments. In this experiment the value of D_M was cycled between 0% and 25% to determine repeatability. As seen in Fig. 4, the conversion, X, for the vertical segment of the experiment was roughly 98.5%. In the second and fourth segments, X values of approximately 98.2% and 97.8%, were obtained, respectively. Segments three and five, with $D_M = 25\%$, yielded the

Table 1
Summary of experimental results.

Experiment/segment	Reactor angle, °	Oil flow, L/min	Methoxide flow, L/min	Methoxide diversion, %	Triglyceride conversion, %	Glycerin separation, %
1						
2 h 1	0	0.92	0.22	0	98.93 ± 0.13	70 ± 8
4 h 2	45	0.94	0.22	0	98.04 ± 0.20	98 ± 4
3 h 3	45	0.91	0.22	25	99.18 ± 0.14	85 ± 11
2						
3 h 1	0	0.94	0.23	0	98.55 ± 0.14	N/A
3 h 2	45	0.94	0.23	0	98.23 ± 0.20	N/A
3 h 3	45	0.95	0.22	25	98.63 ± 0.17	N/A
3 h 4	45	0.96	0.22	0	97.75 ± 0.23	N/A
3 h 5	45	0.95	0.22	25	98.72 ± 0.19	N/A
3						
3 h 1	0	0.92	0.22	0	98.44 ± 0.34	72 ± 2
3 h 2	45	0.94	0.22	0	96.15 ± 0.99	86 ± 2
3 h 3	45	0.96	0.22	25	98.96 ± 0.35	89 ± 8
3 h 4	45	0.94	0.22	0	97.71 ± 0.64	92 ± 2
3 h 5	45	0.95	0.22	25	99.45 ± 0.19	94 ± 2
3 h 6	45	1.04	0.243	0	98.65 ± 0.16	85 ± 4

Table 2
GC results for experiment 1. The conversion and bound glycerin results are averages of 3 measurements taken on the sample collected at each hour, followed by the standard deviation.

Experiment 1				
Segment	Time (h)	% Conversion, X	Bound glycerin	ASTM result
1 (90°)	1	99.013 ± 0.0681	0.145 ± 0.0091	Pass
	2	98.837 ± 0.1102	0.163 ± 0.0104	Pass
2 (45°)	3	98.14 ± 0.1595	0.241 ± 0.0179	Fail
0%	4	98.092 ± 0.0285	0.235 ± 0.0032	Pass
Methoxide diversion	5	98.06 ± 0.1626	0.244 ± 0.007	Fail
	6	97.852 ± 0.2954	0.251 ± 0.0165	Fail
3 (45°)	7	99.233 ± 0.0740	0.103 ± 0.0084	Pass
25%	8	99.245 ± 0.1310	0.104 ± 0.0154	Pass
Methoxide diversion	9	99.073 ± 0.1669	0.126 ± 0.0148	Pass

Table 3
Glycerol separation efficiencies estimated for each segment of experiment 1.

Parameter	Segment 1	Segment 2	Segment 3
Glycerin production, F_{GP}, g/s	1.43 ± 0.015	1.44 ± 0.015	1.41 ± 0.015
Glycerin recovery, F_{GS}, g/s	0.995 ± 0.11	1.42 ± 0.062	1.20 ± 0.16
Glycerin separation efficiency, G_E, %	69.8 ± 7.9	98.0 ± 4.4	85.1 ± 11.2

highest values of X, approximately 98.7%. Similar to experiment 1, the segments where the reactor was vertical, or where the reactor was tilted with methoxide diversion, provided ASTM quality biodiesel.

In segment four, where the reactor was tilted with $D_M = 0$, two of the three samples failed the free and total glycerin test (Table 4). The samples from segment two passed the free and total glycerin test even without methoxide diversion, although the bound glycerin results in Table 4, below, indicate that those samples were close to the bound glycerin limit of 0.24. Experiment 2 showed that the methoxide diversion to the top injection location of the reactor could be switched on and off without causing negative disturbances

Table 4
GC results for experiment 2. The conversions and bound glycerin results are the averages of 3 measurements conducted with each hourly sample.

Experiment 2				
Segment	Time (h)	% Conversion, X	Bound glycerin	ASTM result
1 (90°)	1	98.525 ± 0.0566	0.167 ± 0.0090	Pass
	2	98.549 ± 0.1042	0.167 ± 0.0098	Pass
	3	98.582 ± 0.2469	0.158 ± 0.0124	Pass
2 (45°)	4	98.281 ± 0.2677	0.196 ± 0.0150	Pass
0%	5	98.303 ± 0.0728	0.194 ± 0.0072	Pass
Methoxide diversion	6	98.099 ± 0.2102	0.209 ± 0.0101	Pass
3 (45°)	7	98.650 ± 0.1125	0.143 ± 0.0060	Pass
25%	8	98.699 ± 0.1800	0.143 ± 0.0095	Pass
Methoxide diversion	9	98.550 ± 0.2199	0.165 ± 0.0125	Pass
4 (45°)	10	97.774 ± 0.2855	0.246 ± 0.0163	Fail
0%	11	97.667 ± 0.3141	0.249 ± 0.0146	Fail
Methoxide diversion	12	97.822 ± 0.1276	0.237 ± 0.0078	Pass
5 (45°)	13	98.695 ± 0.2075	0.138 ± 0.0031	Pass
25%	14	98.904 ± 0.0493	0.126 ± 0.0087	Pass
Methoxide diversion	15	98.553 ± 0.1057	0.153 ± 0.0091	Pass

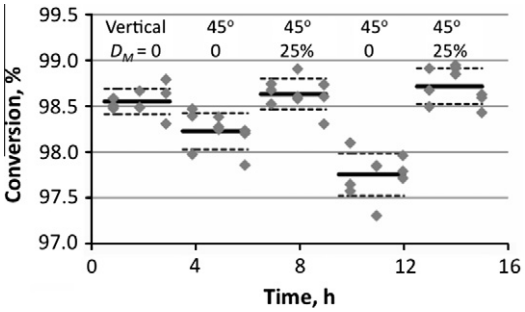

Fig. 4. Experiment 2. Conversion vs. Time. Each conversion data point is displayed, along with the average conversion attained during each segment of the experiment. The standard deviations of the data in each segment of the experiment are also displayed as dotted lines above and below the solid line representing the average value of the conversion.

in reactor performance. The biodiesel produced in the reactor/separator at 45° with the diversion turned on passed the ASTM free and total glycerin test in every instance by a wide margin.

The glycerin separation efficiency was not calculated for this experiment due to failure of an instrument not detected until after the completion of the experiment. Detailed data on separation efficiency is given below in experiment 3 and in previous work [21].

3.3. Experiment 3

Experiment 3 was designed to determine if glycerin separation efficiency, G_E, was affected with the new methoxide diversion adjustment. Preliminary data were also acquired at increased flows of waste vegetable oil and methoxide. Fig. 5a shows that the trends regarding X from the first two experiments were also observed in experiment 3. The vertically run segment achieved X values between 98% and 99% and every sample passed the free and total glycerin test (Table 5). With the reactor tilted to 45°, and $D_M = 0$, X values were nearly all below 98%, and all samples but one failed the ASTM free and total glycerin test (Table 5). With the reactor tilted to 45°, and $D_M = 25\%$, nearly all the X values were above 99%, and every sample passed the free and total glycerin test.

Fig. 5b shows that at 45°, G_E increases in comparison to the value seen at 90°, as noted previously [21]. There is little effect of D_M on G_E as the data for segments 2–4 show little fluctuation in G_E, and consistently separate more than 80% of the glycerin. Thus, the strategy of diverting 25% of the methoxide to the upper injector increases the conversion, allows the produced biodiesel to pass ASTM standards, and preserves the high glycerin separation efficiency of the tilted reactor. With G_E approaching 90%, the glycerol removal units required in all other biodiesel production systems are not required here since the small amount of remaining glycerin is easily removed in other downstream processing operations.

The final segment of experiment 3 was devoted to running the reactor at a 45° angle without any methoxide diversion, and a 10% increase in the total flows of waste vegetable oil and methoxide. The flow of vegetable oil was increased from 0.95 L/min to 1.05 L/min, and the flow of methoxide was increased from 0.22 L/min to 0.242 L/min. As seen in Fig. 5a and b, G_E for this segment was similar to the 85% glycerin separation efficiency observed in segment 2, while X held steady at approximately at 98.6% for the 3 h segment. All samples collected during this final segment passed the ASTM free and total glycerin test.

The results of the final segment of experiment 3 are surprising since most other biodiesel produced with the reactor tilted at 45° and $D_M = 0$ did not pass the free and total glycerin ASTM test. Moreover, the increased flow used in the final segment of experiment 3 was expected to decrease the conversion below that seen

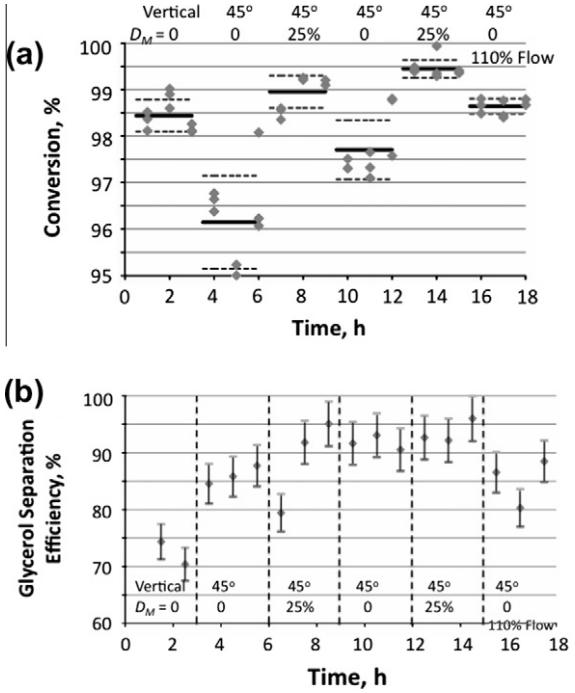

Fig. 5. (a) Experiment 3. Conversion vs. Time. Each conversion data point is displayed, along with the average conversion attained during each segment of the experiment. The standard deviations of the data in each segment of the experiment are also displayed as dotted lines above and below the solid line representing the average value of the conversion. (b) Glycerin separation efficiency from experiment 3 according to Eqs. (2)–(4). Data points appear on the half-hour as separation efficiency is the averaged value over each 1 h time period. There was no data at early times for separation so an average value over the first hour is not reported.

Table 5
GC results for experiment 3. The results are the averages of 3 measurements.

Experiment 3				
Segment	Time	% Conversion	Bound glycerin	ASTM result
1 (90°)	1	98.334 ± 0.2045	0.194 ± 0.0095	Pass
	2	98.840 ± 0.2149	0.132 ± 0.0051	Pass
	3	98.156 ± 0.0904	0.192 ± 0.0090	Pass
2 (45°)	4	96.596 ± 0.1981	0.346 ± 0.0211	Fail
0%	5	95.066 ± 0.1449	0.436 ± 0.0874	Fail
Methoxide diversion	6	96.791 ± 1.1164	0.358 ± 0.1349	Fail
3 (45°)	7	98.508 ± 0.1336	0.160 ± 0.0067	Pass
25%	8	99.228 ± 0.0233	0.093 ± 0.0021	Pass
Methoxide diversion	9	99.133 ± 0.0599	0.105 ± 0.0046	Pass
4 (45°)	10	97.375 ± 0.1174	0.262 ± 0.0140	Fail
0%	11	97.360 ± 0.2807	0.275 ± 0.0148	Fail
Methoxide diversion	12	98.387 ± 0.7006	0.174 ± 0.0752	Pass
5 (45°)	13	99.439 ± 0.0497	0.075 ± 0.0050	Pass
25%	14	99.529 ± 0.3583	0.082 ± 0.0044	Pass
Methoxide diversion	15	99.379 ± 0.0300	0.080 ± 0.0046	Pass
6 (45°)	16	98.652 ± 0.1570	0.155 ± 0.0072	Pass
0% Methoxide diversion	17	98.534 ± 0.2003	0.154 ± 0.0078	Pass
110% Total flow	18	98.751 ± 0.0686	0.143 ± 0.0093	Pass

for similar operating conditions at lower flows because increasing the flows reduces the residence time and thus decreases time for reaction. While X and G_E did decrease relative to the segment of experiment 3 immediately preceding the final segment, these performance measures did not change as much as expected. This data at higher flows suggests that the reactor/separator operation and performance may be optimized further, perhaps with a combination of methoxide diversion and increased flow rates.

3.4. Overall reactor performance

A concise summary of product quality in terms of the ASTM free and total glycerin test is given in Fig. 6 for the operating conditions of: vertical with no methoxide diversion, 45° angle with no methoxide diversion, and 45° angle with 25% methoxide diversion. The data from segment 6 of experiment 3 is omitted as it was obtained under different operating conditions. Fig. 6 illustrates that the reactor may be operated reliably with a 45° tilt angle if a portion of the injected methoxide is diverted to an upper injection location. Additional fine-tuning is required to optimize the diversion ratio and reinjection location. Moreover, the separation efficiency results indicate that very little if any separation efficiency is lost due to the methoxide diversion.

4. Discussion and reactor model

In an attempt to understand the behavior of the reactor/separator, a simple countercurrent flow, equilibrium model was used to perform calculations. To overcome the considerable difficulties in modeling the flow and reaction mediated glycerol nucleation, coalescence, and droplet size distribution behavior [27–33], the glycerin was modeled with a simple partition mechanism. While this approach is certainly an oversimplification of very complex behavior, it does permit the model to emulate many of the trends observed in the data. Due to the tedious calculations, only the first 15 cm of the reactor are modeled below, and the long tail of the conversion curve as well as a detailed optimization study will be presented separately.

The glycerin partitions into a fraction within the oil phase that may exist as free molecules or the very small droplets that are too small to settle, and a fraction within the glycerol phase which settles countercurrently to the upwelling oil phase. A schematic diagram of the model is shown in Fig. 7, depicting a small section of the reactor of length Δz. Methanol also partitions between the oil phase and the glycerol phase. The oil phase is modeled as a 4-component reacting fluid consisting of triglycerides, biodiesel, methanol and glycerin, and the molar flows of each species in the oil phase are denoted by $\dot{n}_i^o$ in Fig. 7. The glycerol phase is modeled as a 2-component fluid consisting of methanol and glycerin, denoted by $\dot{n}_i^g$ in Fig. 7. The chemical reactions are modeled with a single, reversible global reaction obtained by combining the sequential reactions R.1–R.3,

$$\mathrm{TG} + 3\ \mathrm{MeOH} \rightleftharpoons 3\ \mathrm{FAME} + \mathrm{G} \tag{R.4}$$

Detailed analysis of the reaction mechanism indicates the overall reaction is first order in each of the major species, leading to a kinetic description that is reversible and second order [34],

$$\frac{d[TG]}{dt} = -k\{[TG][\mathrm{MeOH}] - \frac{1}{K}[\mathrm{FAME}][G]\} \tag{5}$$

An explicit dependence on catalyst loading would improve the model, and limited work indicates that the dependence on the KOH catalyst is first order [34], but this model does not track the catalyst in the reactor. Many kinetics models exist for these reactions [35–41], but this simplified expression is sufficient to demonstrate the trends seen experimentally.

The flows and compositions of the oil and glycerol phases are obtained by solving the mole balances for all the species. The model assumes that the flows and compositions of the oil and glycerol phases are known at the bottom of the reactor, and the goal of the

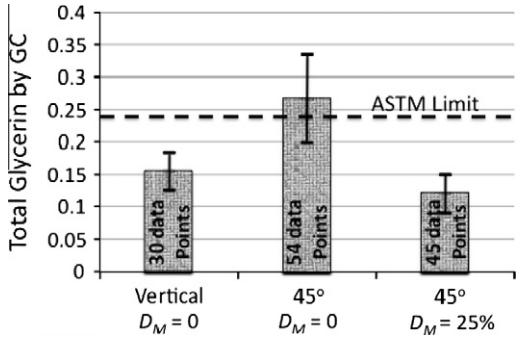

Fig. 6. Summary of experimental GC measurements in terms of the ASTM free and total glycerin test, for the 3 experiments reported above and for data from Unker et al. [21].

model is to integrate the model equations up the length of the reactor. The change in the molar flow of triglycerides due to chemical reaction, over a length Δz of the reactor, is obtained from Eq. (5) as,

$$\Delta \dot{r}_{TG} = \frac{d[TG]}{dt} \cdot \frac{\pi R^2 \Delta z}{MW_o} \tag{6}$$

where R is the radius of the reactor and $\Delta \dot{r}_{TG} < 0$. The species balances on TG and FAME include only oil phase flows since it is assumed that TG and FAME do not partition into the glycerol phase. Thus,

$$\dot{n}^o_{TG}\big|_{z+\Delta_z} = \dot{n}^o_{TG}\big|_z + \Delta \dot{r}_{TG}\big|_z \tag{7}$$

$$\dot{n}^o_{\mathrm{FAME}}\big|_{z+\Delta_z} = \dot{n}^o_{\mathrm{FAME}}\big|_z - 3\Delta \dot{r}_{TG}\big|_z \tag{8}$$

where the reaction stoichiometry indicates that 3 mol of FAME will be produced for each mole of TG consumed. For simplicity, the reaction rate is evaluated at location z, although implicit numerical schemes could average the reaction rates at z and $z + \Delta z$. The mole balance equations for MeOH and G are more complicated since they include flows in both the oil phase and the glycerol phase. Thus,

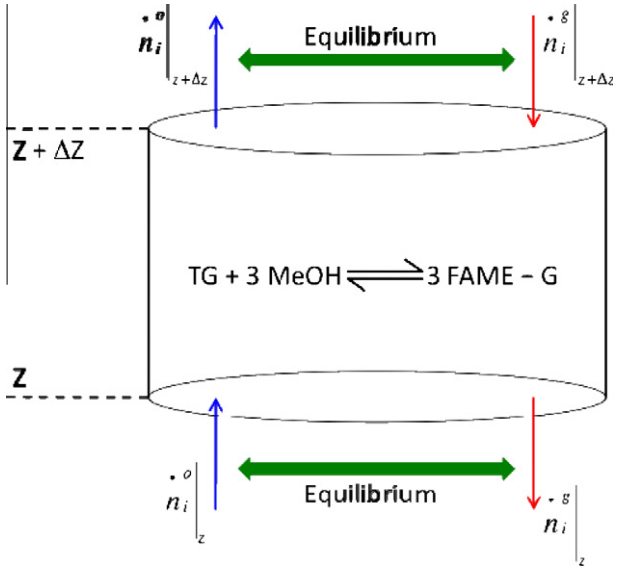

Fig. 7. Schematic illustration of the flow, reaction, and equilibrium model of the continuous reactor/separator. The molar flows of the upward flowing components of the oil phase are represented by $\dot{n}^o_i$ at location z and location $z + \Delta z$. The molar flows of the downward flowing components of the glycerol phase are represented by $\dot{n}^g_i$ at location z and location $z + \Delta z$.

$$\dot{n}^o_{\mathrm{MeOH}}\big|_{z+\Delta_z} + \dot{n}^g_{\mathrm{MeOH}}\big|_z = \dot{n}^o_{\mathrm{MeOH}}\big|_z + \dot{n}^g_{\mathrm{MeOH}}\big|_{z+\Delta z} + 3\Delta \dot{r}_{TG}\big|_z \tag{9}$$

$$\dot{n}_G{}^o\big|_{z+\Delta_z} + \dot{n}_G{}^g\big|_z = \dot{n}_G{}^o\big|_z + \dot{n}_G{}^g\big|_{z+\Delta_z} - \Delta \dot{r}_{TG}\big|_z \tag{10}$$

where the reaction stoichiometry indicates that 3 mol of MeOH will be consumed for each mole of TG consumed and that 1 mol of G will be produced for each mole of TG consumed. Since all the molar flows and concentrations are known at location z, Eqs. (9) and (10) contain 4 unknowns, the molar flows of methanol and glycerin in both the oil and glycerol phases at location $z + \Delta z$.

Requiring that the oil and glycerol phases be in equilibrium at all z locations provides the additional 2 equations required to find all the molar flows at $z + \Delta z$. This equilibrium requirement is expressed in terms of binary partition coefficients for methanol and glycerin. The partition coefficients are defined as the species mole fraction in the glycerol phase, x^g_i, divided by the species mole fraction in the oil phase, x^o_i, where the species, i, is either methanol or glycerin. The partition coefficients, evaluated at $z + \Delta z$, are,

$$K_M = \frac{x^g_{\mathrm{MeOH}}|_{z+\Delta z}}{x^o_{\mathrm{MeOH}}|_{z+\Delta z}} = \left.\frac{\dot{n}^g_{\mathrm{MeOH}}/(\dot{n}^g_{\mathrm{MeOH}} + \dot{n}^g_G)}{\dot{n}^o_{\mathrm{MeOH}}/(\dot{n}^o_{TG} + \dot{n}^0_{\mathrm{FAME}} + \dot{n}^o_{\mathrm{MeOH}} + \dot{n}^o_G)}\right|_{z+\Delta z} \tag{11}$$

$$K_G = \frac{x^g_G|_{z+\Delta z}}{x^o_G|_{z+\Delta z}} = \left.\frac{\dot{n}^g_G/(\dot{n}^g_{\mathrm{MeOH}} + \dot{n}^g_G)}{\dot{n}^o_G/(\dot{n}^o_{TG} + \dot{n}^0_{\mathrm{FAME}} + \dot{n}^o_{\mathrm{MeOH}} + \dot{n}^o_G)}\right|_{z+\Delta z} \tag{12}$$

where the mole fractions are expressed in terms of the molar flows. Variations of K_M and K_G alter the quantitative results of the model but do not change the trends illustrated below. We recognize that simple binary partition coefficients change with composition in multi-component systems. An important point to note is the large change in methanol partitioning between glycerol and triglycerides relative to partitioning between glycerol and biodiesel. The experimental system includes a static mixer primary injection system specifically to allow roughly 20% conversion of triglycerides to biodiesel prior to entering the laminar flow reactor/separator. Thus, the feed stream that is in equilibrium with the exiting glycerol stream is at 20% triglyceride conversion, and the partition coefficients are assumed constant throughout the reactor as conversion further increases.

Solving Eqs. (9)–(12) for the methanol and glycerin molar flows in both the glycerol and oil phases requires an iterative procedure. Due to the presence of the chemical reaction, multiple roots and high sensitivity increased the difficulty of the solution procedure. Therefore, only the bottom 15 cm portion of the reactor has been successfully simulated at this time. Nevertheless, this lower portion of the reactor is the region where much of the chemical conversion occurs and where much of the interphase mass transfer occurs. The preliminary modeling results therefore provide insight into the experimental results and are presented at this time in lieu of more complete modeling results under development.

Table 6 summarizes the parameters used to generate the curves shown below. The model requires the estimation of the volumetric flow of the oil phase to compute the molar concentrations within the oil phase to calculate reaction rate, and the measured oil phase density was used for this purpose. The reaction, mass balance and equilibrium relationships are solved for the molar flows in both phases at successive steps up the reactor column.

Fig. 8a shows the profiles of triglyceride conversion and oil phase methanol molar flow as a function of position in the reactor for the case where 90% of the produced glycerin is recovered and for the case where 70% of the produced glycerin is recovered, emulating the 45° tilted reactor with no methoxide diversion and the vertical reactor, respectively. The model correctly simulates the small reduction in conversion observed in the experimental data for the case of the higher glycerin separation efficiency obtained with the tilted reactor. The curves of methanol flow in the oil phase

Table 6
Parameters used in the model to describe experimental data.

Reaction rate constant, k, cc/mol-s	Reaction equilibrium constant, K	Methanol partition coefficient, K_M	Glycerin partition coefficient, K_G	Oil phase density, ρ_o, g/cc
5	81	0.96138	9.0427	0.88

provide insight into that experimental result by indicating that the oil phase methanol concentration is expected to be lower when a larger fraction of glycerin is recovered. A lower methanol concentration slows the forward reaction.

While a larger glycerin recovery reduces the methanol concentration in the oil phase, it also reduces the glycerin concentration in the oil phase. A reduction of oil-phase glycerin concentration reduces the rate of the reverse reaction, increasing conversion. However, the oil phase glycerin concentration was quite low in both cases due to strong partitioning of glycerin to the glycerol phase. In the experiments conducted and in these initial modeling results, the reduction in methanol is therefore much more significant than the reduction in glycerin, leading to the reduction in conversion observed experimentally and in the model results of Fig. 8a.

Fig. 8b shows the simulated change in triglyceride conversion when the flow is increased to 110% of the nominal flows, as was done in segment 6 of experiment 3. In the experimental work, the glycerin separation efficiency decreased as the flow increased, but in the simulation, the effects of flow and of glycerin separation can be separated. Thus, the middle curve is the triglyceride conversion at the nominal flow and at 90% glycerin separation (same as Fig. 8a). The dashed curve illustrates that the expected conversion is expected to slightly decrease if the flow is increased to 110% of nominal and the glycerin separation remains at 90%. However, the uppermost curve indicates that the drop in glycerin separation efficiency observed experimentally, caused by the increase in flow, more than compensates for the direct effect of the flow on triglyceride conversion. The model indicates that the conversion can actually increase when the flow increases, in accordance with the observed increase in conversion seen in segment 6, compared to segments 2 and 4, of experiment 3. This result is not expected to hold over a wide range of flows, but does indicate that increased flow can carry additional methanol up the reactor to increase the conversion.

The effects of diverting a portion of the methoxide to an upper injection location are illustrated in Fig. 9. Fig. 9a shows the curves of triglyceride conversion and oil phase methanol flow for the cases of $D_M = 0\%$, 10% and 25%, all with 90% glycerol recovery. Reducing the methanol concentration in the lower part of the reactor reduces conversion, and adding methanol at the intermediate location then increases conversion. Interestingly, the model indicates that diverting methanol to the upper injection location leads to higher overall conversions. Fig. 9b emphasizes this point by plotting the conversions for the cases with 90% glycerin separation (tilted reactor) divided by the conversion for the case with 70% glycerin separation (vertical reactor). Thus, we observe that in the case with no methanol diversion, the conversion drops to about 95% of the conversion for the vertical reactor, and then very gradually increases towards the conversion of the vertical reactor. However, in the case of 25% methanol diversion, the conversion drops to only about 82% of the conversion of the vertical reactor before the diverted methanol is injected, and then climbs rapidly. The conversion with 25% methanol diversion surpasses the conversion for the case of no diversion, as seen experimentally, and climbs to the same conversion as seen in the vertical reactor. Clearly, Fig. 9b indicates that the conversion with 25% diversion will surpass that seen in the vertical reactor in a longer simulated reactor.

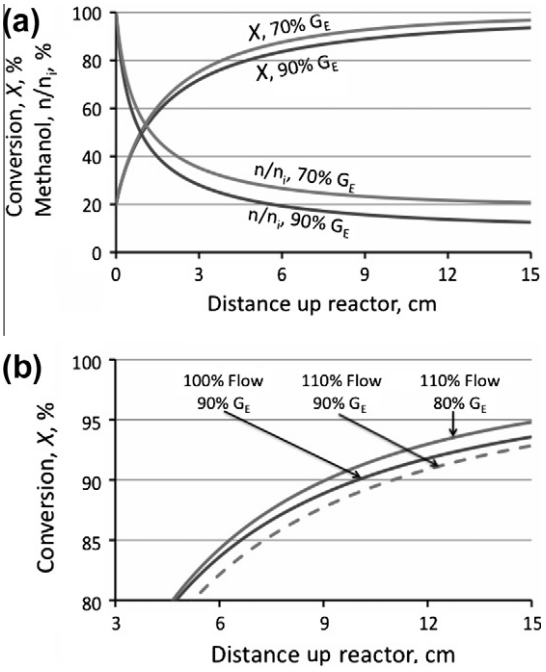

Fig. 8. (a) Triglyceride conversion, X, and dimensionless oil phase methanol flow, n/n_i, at various axial locations, simulating the differences between a vertical reactor achieving roughly 70% glycerin separation, and a 45° reactor achieving roughly 90% glycerin separation, without methoxide diversion. (b) Triglyceride conversion, X, in a 45° reactor at various axial locations, simulating the effects of increasing the flow of both the oil feed and the methoxide feed by 10%.

The model simulates all the major trends observed in the experiments, indicating that the experimental results are consistent with basic mass balance and phase equilibrium requirements. The simplified model can aid in explaining the data and has limited use in design optimization, however, the simplified model requires specification of the glycerol separation efficiency, G_E. In order to predict G_E, the much more challenging modeling issues of nucleation, coalescence, and droplet size distribution of the glycerol phase need to be addressed.

5. Summary

Three independent experiments were run to test a reactant injection strategy designed to improve the performance of a biodiesel reactor/separator. The experiments showed that injecting 25% of the total methoxide flow at a location 2/3 of the distance up the reactor maintained high glycerin separation efficiencies while increasing the triglyceride conversion to levels easily meeting ASTM specifications. Experiments 1 and 2 showed that diverting 25% of the methoxide can be switched on and off without disturbing reactor performance. Experiment 3 showed that a high level of glycerin separation was maintained during the methoxide diversion while still producing ASTM quality biodiesel. Experiment 3 also yielded preliminary results regarding reactor performance at increased flow rates that suggest that the reactor/separator can be further optimized in the future.

A model of the reactor/separator that assumes phase equilibrium between the upward flowing oil phase and the downward flowing glycerol phase simulated all the major trends observed in the experimental conversion measurements, including the effects of tilting the reactor, diverting a portion of the methoxide injection to an upper injector, and increasing the reactant flows. The insight

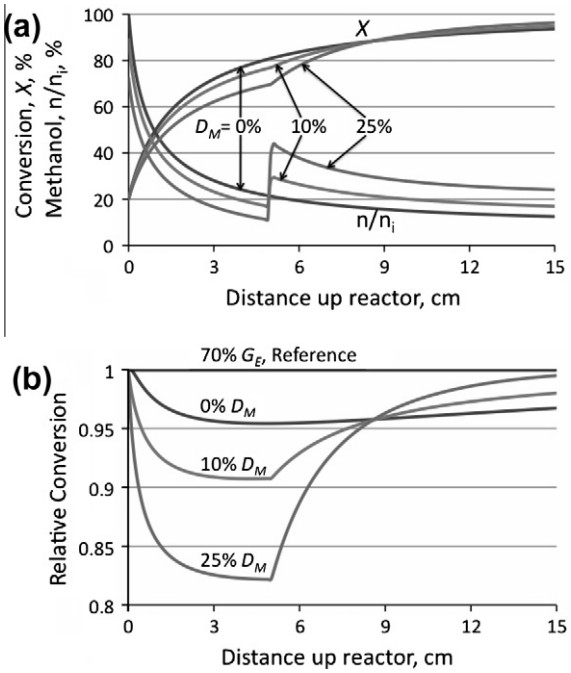

Fig. 9. (a) Conversion, X, and dimensionless oil-phase methanol flow, n/n_i, for various levels of methoxide diversion, D_M, from the lower injection location to the upper injection location. (b) Conversion at various levels of methoxide diversion in the tilted reactor with 90% glycerin separation, G_E, relative to conversion for the vertical reactor with G_E = 70%.

provided by the model indicates that the critical parameter is the methanol flow in the oil phase, and that operational changes that increase that flow will increase conversion. Thus, increasing total reactant flows into the reactor actually increased chemical conversion slightly because the increased flow carried more methanol up the reactor tube via a mechanism coupled to the glycerin separation efficiency.

Acknowledgements

The authors gratefully acknowledge the support of DOE Grant DE-EE0003116. RSP is grateful for summer support from Sichuan University, Chengdu, China. UConn students Salvatore Delucia, Alyssa Midgette and Karan Ojha worked for many hours in the laboratory to help run the experiments.

References

[1] Meher LC, Vidya Sagar D, Naik SN. Technical aspects of biodiesel production by transesterification – a review. Renew Sustain Energy Rev 2006;10:248–68.
[2] Sharma YC, Singh B, Upadhyay SN. Advancements in development and characterization of biodiesel – a review. Fuel 2008;87:2355–73.
[3] Murugesan A, Subramanian R, Nedunchezhian N. Biodiesel as an alternative fuel for diesel engines – a review. Renew Sustain Energy Rev 2009;13:653–62.
[4] Lu H, Liu Y, Zhou H, Yang Y, Chen M, Liang B. Production of Biodiesel from *Jatropha Curcas* L. Oil Comput Chem Eng 2009;33(5):1091–6.
[5] Dreger EE. Method of treating fatty glycerides. US Patent No. 2383,596; 1945.
[6] Bradshaw GB. Meuly WC. Process of making pure soaps. US Patent No. 2271,619; 1942.
[7] Darnoko D, Cheryan M. Continuous production of palm methyl esters. J Am Oil Chem Soc 2009;77:1269–72.
[8] Fleisher CA. Continuous transesterification process. US Patent 7145,026; 2006.
[9] Thompson JC, He BB. Biodiesel production using static mixers. Am Soc Agri Biol Eng 2007;50:161–5.
[10] Jiang W, Lu H, Qi T, Yan S, Liang B. Preparation, application, and optimization of Zn/Al complex oxides for biodiesel production under sub-critical conditions. Biotechnol Adv 2010;28:620–7.
[11] Peterson CL, Cook JL, Thompson JC, Taberski JS. Continuous flow biodiesel production. Appl Eng Agri 2002;18:5–11.
[12] Kraai GN, Schuur B, van Zwol F, Van de Bovenkamp HH, Heeres HJ. Novel highly integrated biodiesel production technology in a centrifugal contactor separator device. Chem Eng J 2009;154(1–3):384–9.
[13] Kiss AA, Dimian AC, Rothenberg G. Biodiesel by catalytic reactive distillation powered by metal oxides. Energy Fuels 2008;22:598–604.
[14] Noshadi I, Amin NAS, Parnas RS. Continuous production of biodiesel from waste cooking oil in a reactive distillation column catalyzed by solid heteropolyacid: optimization using response surface methodology (RSM). Fuel 2012;94:156–64.
[15] Sarkar S, Mumford CJ, Phillips CR. Liquid–liquid extraction with interphase chemical reaction in agitated columns. Ind Eng Chem Process Dev 1980: 665–71.
[16] Lux S, Winkler T, Siebenhofer M. Synthesis and isolation of methyl acetate through heterogeneous catalysis with liquid–liquid extraction. Ind Eng Chem Res 2010;49:10274–8.
[17] Minotti M, Doherty MF, Malone MF. Design for simultaneous reaction and liquid–liquid extraction. Ind Eng Chem Res 1998;37:4748–55.
[18] Van Gerpen J. Biodiesel processing and production. Fuel Process Technol 2005;86:1097–107.
[19] Parnas R.S. Weed C. Leadbeater N. Boucher M. Methods and systems for alkyl ester production. US Patent 7544,830; 2009.
[20] Boucher MB, Weed C, Leadbeater NE, Wilhite BA, Stuart JD, Parnas RS. Pilot scale two-phase continuous flow biodiesel production via novel laminar flow reactor-separator. Energy Fuels 2009;23:2750–6.
[21] Unker SA, Boucher MB, Hawley KR, Midgette AA, Stuart JD, Parnas RS. Investigation into the relationship between the gravity vector and the flow vector to improve performance in two-phase continuous flow biodiesel reactor. Bioresour Technol 2010;101:7389–96.
[22] Mitrovic B, Parekh A, Ramer J, Merai V, Armour EA, Kadinski L, et al. Reactor design optimization based on 3D modeling of nitrides deposition in MOCVD vertical rotating disc reactors. J Cryst Growth 2006;289:708–14.
[23] Taboada-Serrano P. Szymcek P. McCallum , SD. Tsousis C. A novel continuous-flow reactor for gas hydrate production. In: 6th International conference on gas hydrates. ICGH; 2008.
[24] Boucher M, Unker S, Hawley K, Wilhite B, Stuart J, Parnas RS. Variables affecting homogeneous acid catalyst recoverability and reuse after esterification of concentrated omega-9 polyunsaturated fatty acids in vegetable oil triglycerides. Green Chem 2008;10(12):1331–6.
[25] Darnoko D, Cheryan M. Kinetics of palm oil transesterification in a batch reactor. J Am Oil Chem Soc 2000;77:1263–7.
[26] Asakuma Y, Maeda K, Kuramochi H, Fukui K. Theoretical study of the transesterification of triglycerides to biodiesel fuel. Fuel 2009;88(5):786–91.
[27] Hohenberg PC, Halperin BI. Theory of dynamic critical phenomena. Rev Mod Phys 1977;49(3):435.
[28] Bates PW, Fife PC. The dynamics of nucleation for the Cahn–Hilliard equation. SIAM J Appl Math 1993;53:990.
[29] Bray AJ. Theory of phase-ordering kinetics. Adv Phys 1994;43(3):357–459.
[30] Badalassi VE, Ceniceros HD, Banerjee S. Computation of multiphase systems with phase field models. J Comput Phys 2003;190:371–97.
[31] Kim J, Kang K, Lowengrub J. Conservative multigrid methods for ternary Cahn–Hilliard systems. Commun Math Sci 2004;2:53–77.
[32] Aarts DGAL, Lekkerkerker HNW, Guo H, Wegdam GH, Bonn D. Hydrodynamics of droplet coalescence. Phys Rev Lett 2005;95:164503.
[33] Khatavkar VV, Anderson PD, Meijer HEH. On scaling of diffuse-interface models. Chem Eng Sci 2006;61:2364–78.
[34] Boucher MB. Variable feedstock biodiesel synthesis via novel laminar flow reactor/separator. MS thesis, University of Connecticut; 2008.
[35] Freedman B, Butterfield RO, Prye EH. Tansesterification kinetics of soybean oil. J Am Oil Chem Soc 1986;10:1375.
[36] Noureddini H, Zhu D. Kinetics of transesterification of soybean oil. J Am Oil Chem Soc 1997;74:1457.
[37] Komers K, Skopal F, Stloukal R, Machek J. Kinetics and mechanism of KOH catalyzed methanolysis of rapeseed oil for biodiesel production. Eur J Lipid Sci Technol 2002;104:728.
[38] Casas A, Ramos MJ, Pérez T. Kinetics of chemical interesterification of sunflower oil with methyl acetate for biodiesel and triacetin production. Chem Eng J 2011;171(3):1324–32.
[39] Vicente G, Martınez M, Aracil J, Esteban A. Kinetics of sunflower oil methanolysis. Ind Eng Chem Res 2005;44:5447.
[40] Karmee SK, Chandna D, Ravi R, Chadha A. Kinetics of base-catalyzed transesterification of triglycerides from pongamia oil. J Am Oil Chem Soc 2006;83:873.
[41] Bambase M, Nakamura N, Tanaka J, Matsumarai M. Kinetics of hydroxide catalyzed methanolysis of crude sunflower oil for the production of fuel grade methyl esters. J Chem Technol Biotechnol 2007;82:273.